

This item is the archived peer-reviewed author-version of:

Microclimate reveals the true thermal niche of forest plant species

Reference:

Haesen Stef, Lenoir Jonathan, Gril Eva, De Frenne Pieter, Lembrechts Jonas, Kopecky Martin, Macek Martin, Man Matej, Wild Jan, Van Meerbeek Koenraad.-
Microclimate reveals the true thermal niche of forest plant species
Ecology letters - ISSN 1461-0248 - Hoboken, Wiley, 26:12(2023), p. 2043-2055
Full text (Publisher's DOI): <https://doi.org/10.1111/ELE.14312>
To cite this reference: <https://hdl.handle.net/10067/2003990151162165141>

1 **Microclimate reveals the true thermal niche of forest plant species**

2 Running title – Incorporating microclimate into SDMs

3 **Stef Haesen^{1,2}, Jonathan Lenoir³, Eva Gril³, Pieter De Frenne⁴, Jonas J. Lembrechts⁵, Martin**
4 **Kopecký^{6,7}, Martin Macek⁶, Matěj Man^{6,8}, Jan Wild^{6,9}, Koenraad Van Meerbeek^{1,2}**

5 ¹Department of Earth and Environmental Sciences, Celestijnenlaan 200E, 3001 Leuven, Belgium; ²KU
6 Leuven Plant Institute, KU Leuven, Leuven, Belgium; ³UMR CNRS 7058 « Ecologie et Dynamique des
7 Systèmes Anthropisés » (EDYSAN), Université de Picardie Jules Verne, Amiens, France; ⁴Forest & Nature
8 Lab, Department of Environment, Ghent University, Geraardsbergsesteenweg 267, 9090 Melle-
9 Gontrode, Belgium; ⁵Research Group PLECO (Plants and Ecosystems), University of Antwerp, 2610
10 Wilrijk, Belgium; ⁶Institute of Botany of the Czech Academy of Sciences, Zámek 1, CZ-25243, Průhonice,
11 Czech Republic; ⁷Faculty of Forestry and Wood Sciences, Czech University of Life Sciences Prague,
12 Kamýcká 129, CZ-165 21, Prague 6 - Suchdol, Czech Republic; ⁸Department of Botany, Faculty of
13 Science, Charles University, Benátská 2, CZ-128 01 Prague 2, Czech Republic; ⁹ Faculty of Environmental
14 Sciences, Czech University of Life Sciences Prague, Kamýcká 129, CZ, 165 21 Prague 6 - Suchdol, Czech
15 Republic;

16 **e-mail & OrcIDs (* = corresponding author)**

17 Stef Haesen*: stef.haesen@kuleuven.be - <https://orcid.org/0000-0002-4491-4213> - tel. = +32 16 32 24 67

18 Jonathan Lenoir: jonathan.lenoir@u-picardie.fr - <https://orcid.org/0000-0003-0638-9582>

19 Eva Gril: eva.gril@u-picardie.fr - <https://orcid.org/0000-0002-7340-8264>

20 Pieter De Frenne: pieter.defrenne@ugent.be - <https://orcid.org/0000-0002-8613-0943>

21 Jonas J. Lembrechts: lembrechtsjonas@gmail.com - <https://orcid.org/0000-0002-1933-0750>

22 Martin Kopecký: ma.kopecky@gmail.com - <https://orcid.org/0000-0002-1018-9316>

23 Martin Macek: Martin.Macek@ibot.cas.cz - <https://orcid.org/0000-0002-5609-5921>

24 Matěj Man: Matej.Man@ibot.cas.cz - <https://orcid.org/0000-0002-4557-8768>

25 Jan Wild: Jan.Wild@ibot.cas.cz - <https://orcid.org/0000-0003-3007-4070>

26 Koenraad Van Meerbeek: koenraad.vanmeerbeek@kuleuven.be - <https://orcid.org/0000-0002-9260-3815>

27 **Keywords:** species distribution modelling, habitat suitability modelling, ecological niche models,
28 MaxEnt, microclimate, microrefugia, ForestClim, forest plant species, species response curves,
29 understory temperatures

30 **Article type:** Letter

- 31 • *Word count: abstract (149), main text (4999) consisting of introduction (718), methods (1912),*
- 32 *results (562), discussion (1697), and conclusion (110)*
- 33 • *Number of references: 70*
- 34 • *Number of figures: 6 in main text, 3 in supporting information*
- 35 • *Number of tables: 0 in main text, 3 in supporting information*
- 36 • *Number of text boxes: 0 in main text, 4 in supporting information*

37 **Statement of authorship**

38 SH, JL, PDF, JLL, and KVM designed the research. SH performed the data analyses, with contributions
39 from JL, EG, PDF, JLL, MK, MM, MM, JW and KVM. SH wrote the manuscript, with contributions from
40 JL, EG, PDF, JLL, MK, MM, MM, JW and KVM. All authors contributed substantially to revisions.

41 **Data accessibility statement**

42 The data and code that support the findings of this study are openly available in Figshare
43 at <https://doi.org/10.6084/m9.figshare.23277332>.

44 **ABSTRACT**

45 Species distributions are conventionally modelled using coarse-grained macroclimate data measured
46 in open areas, potentially leading to biased predictions since most terrestrial species reside in the
47 shade of trees. For forest plant species across Europe, we compared conventional macroclimate-based
48 species distribution models (SDMs) with models corrected for forest microclimate buffering. We show
49 that microclimate-based SDMs at high spatial resolution outperformed models using macroclimate
50 and microclimate data at coarser resolution. Additionally, macroclimate-based models introduced a
51 systematic bias in modelled species response curves, which could result in erroneous range shift
52 predictions. Critically important for conservation science, these models were unable to identify warm
53 and cold refugia at the range edges of species distributions. Our study emphasizes the crucial role of
54 microclimate data when SDMs are used to gain insights into biodiversity conservation in the face of
55 climate change, particularly given the growing policy and management focus on the conservation of
56 refugia worldwide.

57 INTRODUCTION

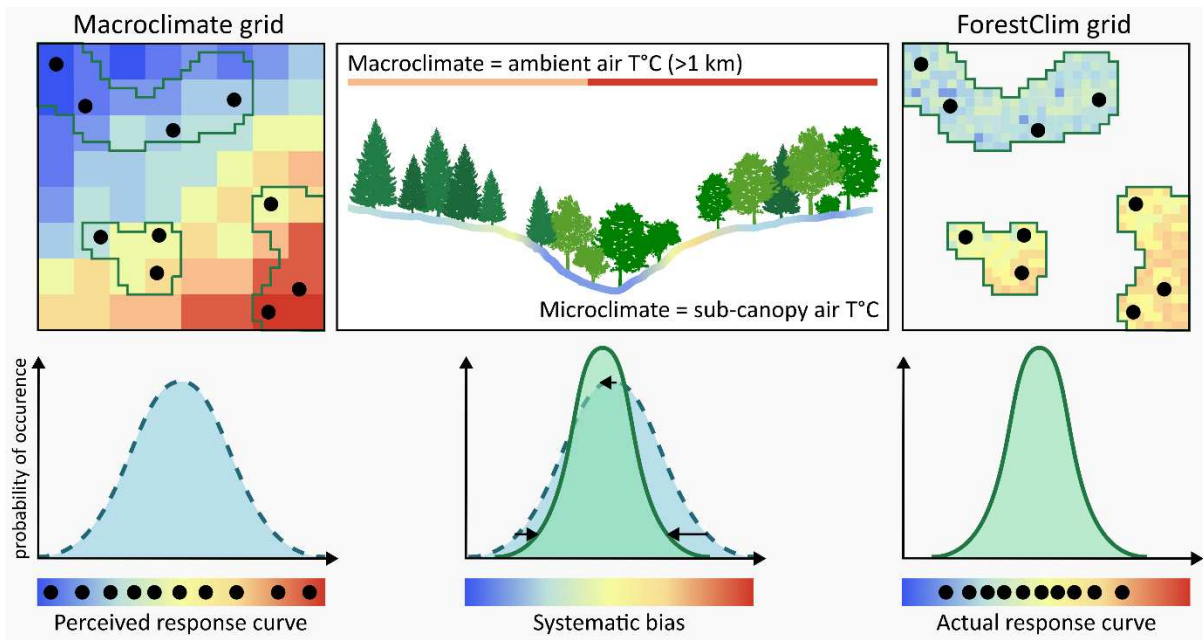
58 Over the last decades, species distribution models (SDMs) have emerged as a central method to
59 project the effects of changing environmental conditions on species' distributions in space and time
60 (Booth et al., 2014; Elith & Leathwick, 2009). Most SDMs are correlative models that infer relationships
61 between species occurrences and the environment using statistical or machine-learning methods
62 (Elith & Leathwick, 2009). Conventional SDM practices involve the incorporation of a standard set of
63 bioclimatic variables with a typical spatial resolution of 30 arc seconds such as in the WorldClim (Fick
64 & Hijmans, 2017) or CHELSA (Karger et al., 2017) datasets. However, these climatological data are
65 derived from standardized meteorological stations at approximately 2 meters height above short
66 grass, exposed to wind, and well away from trees to minimize any noise generated by microclimatic
67 effects (Jarraud, 2008). Gridded macroclimatic data interpolate such weather station data and thus
68 represent the free-air temperature conditions in open ecosystems. Although these data are sufficient
69 to adequately capture changes in free-air temperatures, SDMs based on coarse-scale climate data
70 should be expected to introduce a bias, which stems from the simplified assumptions these models
71 make about the causal relationship between spatially averaged climatic predictors and the fitness of
72 individual organisms (Fourcade et al., 2018). This might be especially problematic when using these
73 data to model the response curves of species that live close to the ground, in topographically
74 heterogeneous terrain, or under trees and shrubs.

75 Variation in microclimates results from physical processes such as airflow and incoming solar
76 radiation interacting with topographic factors such as slope, aspect and surface roughness (Geiger,
77 1950). Additionally, vegetation cover is known to affect local microclimate temperature (De Frenne et
78 al., 2019; Lenoir et al., 2017). Indeed, it is currently well acknowledged that forests harbour distinct
79 microclimatic conditions owing to the structural complexity of the canopy, resulting in shading and
80 evapotranspirative cooling (Geiger, 1950). Forest canopies are characterized by their buffering
81 capacities of extreme temperatures, with cooler sub-canopy maximum temperatures and warmer
82 sub-canopy minimum temperatures in comparison to weather station data (De Frenne et al., 2019).
83 In European forests, this difference can add up to 9°C for mean monthly temperatures (Haesen et al.,
84 2021). There is an urgent need for greater use of fine-scale microclimatic data in ecology as ignoring
85 the mismatch between conventionally-used macroclimatic data and the microclimatic conditions
86 might lead to erroneous predictions, wrong ecological interpretations and, ultimately, questionable
87 conservation decisions (Körner & Hiltbrunner, 2018).

88 This study aims to evaluate the influence of large-scale, gridded microclimate data on the
89 accuracy of SDMs and associated environmental niches and projected geographic ranges of European

90 plant species constrained to forest habitats. Challenging conventional SDMs, we separately tested the
91 effects of using microclimate instead of macroclimate data, as well as of the spatial resolution of these
92 data. To achieve this, we employed three types of SDMs using (1) a macroclimatic dataset at a spatial
93 resolution of $1 \times 1 \text{ km}^2$; (2) an aggregated microclimatic dataset that matched the resolution of the
94 macroclimatic dataset but using sub-canopy microclimate temperatures; and (3) a microclimatic
95 dataset with a spatial resolution of $25 \times 25 \text{ m}^2$, matching the species compositional patterns in the
96 forest understory vegetation and using the microclimate temperatures as perceived below the canopy
97 (Figure 1; Haesen et al., 2023).

98 Forests are recognized for their capacity to moderate temperature, and as such, plant species
99 adapted to forest ecosystems are likely to respond to warmer minimum temperatures and cooler
100 maximum temperatures than those estimated by free-air temperature data collected from weather
101 stations. Therefore, we hypothesized that (1) the actual thermal response curves of forest specialist
102 species are narrower than the thermal response curve as modelled from gridded macroclimate data.
103 We also expect that (2) ranges projected from macroclimate-based models are overestimated,
104 because the presence of a species at locations with distinct microclimates compared to their
105 surroundings may be erroneously attributed to the species' ability to survive in the entire area with
106 that macroclimate. Finally, assuming that species are constrained by the maximum temperature at
107 the southern limit of their latitudinal range and by the minimum temperature at their northern limit,
108 we hypothesized that (3) populations of forest specialist species may survive in local microrefugia,
109 which are cooler than the surrounding landscape at the southern latitudinal limit but warmer than the
110 surrounding area at the northern latitudinal limit.



111

112 *Figure 1: Design of this comparative study, where we compared species distribution models with different set-*
 113 *ups of climatic data. As forests are known to buffer sub-canopy temperatures, forest specialist plant species*
 114 *respond to warmer minimum temperatures and colder maximum temperatures as perceived by the free-air (i.e.*
 115 *macroclimate) temperature data. Therefore, we hypothesize that the actual thermal response curves of forest*
 116 *specialist species, as modelled with the high-resolution ForestClim dataset, would be narrower than the thermal*
 117 *response curve modelled by macroclimate-based SDMs. Note that ForestClim is only available for forest areas,*
 118 *which are delineated by green lines within the simulated grids. Black points indicate species occurrences of a*
 119 *virtual forest plant species (adapted from Lenoir et al., 2017).*

120 **METHODS**

121 **Study area & species selection**

122 Our study area encompasses all 27 EU countries, plus Albania, Andorra, Bosnia and Herzegovina,
123 Kosovo, Liechtenstein, Montenegro, North Macedonia, Norway, San Marino, Serbia, Switzerland and
124 the United Kingdom. The Canary Islands and Azores, as well as Europe's overseas territories were
125 excluded from the analysis.

126 Forest specialist species were selected based on the European forest vascular plant species
127 list (Heinken et al., 2022), which is based on vegetation databases, literature and expert knowledge.
128 From this list, we first selected shrub and herb species, which – unlike tree species – usually complete
129 their entire life cycle within the forest understory layer, thus experiencing forest microclimate
130 dynamics (Caron et al., 2021). Subsequently, we selected the species categorized as forest specialists
131 (i.e., categories 1.1 and 1.2) throughout their entire range, meaning that these species occur only in
132 closed-canopy forests, forest edges or forest openings.

133 **Environmental predictors**

134 Three different sets of bioclimatic temperature-related variables (i.e., macroclimatic data at $1 \times 1 \text{ km}^2$,
135 microclimatic data aggregated at the spatial resolution matching the gridded macroclimate data at 1
136 $\times 1 \text{ km}^2$ and microclimatic data at the native spatial resolution of $25 \times 25 \text{ m}^2$) were used to construct
137 our SDMs, starting from the conventional set of eleven bioclimatic temperature variables. However,
138 we excluded mean temperature of the wettest quarter (BIO8) and mean temperature of the driest
139 quarter (BIO9) as these were recently criticized for their use within species distribution models (Booth,
140 2022). As the available CHELSA and WorldClim data are not fully covering our study period (2000-
141 2020), we used TerraClimate to construct the ‘macroclimatic dataset’ at the typical spatial resolution
142 of $1 \times 1 \text{ km}^2$ as used in conventional SDMs (Abatzoglou et al., 2018). However, TerraClimate bioclimatic
143 variables covering the 2000-2020 period are available at a spatial resolution of $4 \times 4 \text{ km}^2$ and thus
144 were spatially downscaled to a spatial resolution of $1 \times 1 \text{ km}^2$ (Supplementary Methods S1).

145 The ‘microclimatic dataset’ consists of the original bioclimatic variables provided within
146 ForestClim (Haesen et al., 2023), a new high-resolution dataset of forest understory temperature for
147 European forests at a spatial resolution of $25 \times 25 \text{ m}^2$, derived from the ForestTemp model (Haesen
148 et al., 2021). The ‘aggregated dataset’ was generated by averaging the ForestClim bioclimatic variables
149 to a $1 \times 1 \text{ km}^2$ resolution. Note that we did not opt to include a high-resolution topographically
150 downscaled macroclimatic dataset (i.e., $25 \times 25 \text{ m}^2$) within this comparative study as this would turn
151 it into an intermediate ‘mesoclimate’ product, adding extra layers of complexity to the comparative

152 analyses. Besides, the benefit of using topoclimate over macroclimate in SDMs is fairly well covered
153 in the scientific literature (Man et al., 2022).

154 Each set of bioclimatic temperature variables was complemented with six bioclimatic
155 precipitation variables. From the conventional set of eight bioclimatic precipitation variables, we
156 omitted precipitation of the warmest quarter (BIO18) and precipitation of the coldest quarter (BIO19)
157 for similar reasons discussed by (Booth, (2022)). The six bioclimatic precipitation variables were
158 calculated from TerraClimate precipitation data for the 2000-2020 period and disaggregated to match
159 the spatial resolution of each bioclimatic set. Finally, four edaphic variables were added
160 (Supplementary Methods S2), since soil data often increase model performance (Hageer et al., 2017).

161 To reduce overfitting of SDMs, multicollinearity between the predictors was assessed using a
162 pairwise Spearman correlation test (Figure S1). Highly correlated variables (Spearman correlation
163 coefficients > 0.7) were removed from the analysis in order to reach the most parsimonious model
164 (Dormann et al., 2013). When excluding one of the correlated covariate pair, we preferentially
165 retained variables which are known to be more important for plant species distributions (Macek et al.,
166 2019). The final selection of covariates encompassed two temperature variables (maximum
167 temperature of the warmest month (BIO5) and minimum temperature of the coldest month (BIO6)),
168 two precipitation variables (mean annual precipitation, (BIO12) and precipitation seasonality (BIO15))
169 and two edaphic variables (cation exchange capacity and soil clay content). All covariate layers were
170 projected in an equal-area projection (epsg:3035; ETRS89/LAEA).

171 **Species occurrence data**

172 Georeferenced occurrence data were downloaded from the Global Biodiversity Information Facility
173 on the 13th of September 2022 (<https://doi.org/10.15468/dl.kf533a>). To improve data quality for each
174 species, the occurrence data were filtered in the following sequential steps: (1) only records of 'human
175 observations' were selected; (2) records with an unknown coordinate uncertainty or coordinate
176 uncertainty larger than 25 m (i.e., the pixel size) were excluded; (3) records located at country or
177 capital centroids and biodiversity institutions (e.g., botanical gardens) were omitted (Cheng et al.,
178 2021); (4) duplicate records were removed; (5) records outside our study area were deleted; (6) only
179 records observed during our climatic reference period (2000-2020) were selected; (7) records were
180 spatially thinned to one random observation per 25 × 25 m² grid cell; and (8) species with less than 50
181 cleaned occurrence records were omitted, which has been postulated as a minimum standard to build
182 robust SDMs (van Proosdij et al., 2016).

183 Filtering of species occurrence data resulted in a final dataset of 140 species, which are further
184 used for the analyses (Table S1). Note that the same occurrence datasets are needed over the different
185 climatic set-ups to have comparable model outputs. Here, we decided to work with occurrence
186 datasets that underwent a cleaning protocol based upon the characteristics of the microclimatic
187 dataset (i.e., maximum coordinate uncertainty of 25 m, and spatial thinning to a 25 × 25 m² grid cell).

188 **Species distribution modelling**

189 We used MaxEnt, a presence-background algorithm that combines species presence-only data with
190 environmental predictors for the current climate to predict the environmental suitability of each study
191 species across our study area (Phillips et al., 2017). We did that for each of the three sets of bioclimatic
192 variables (i.e., the macroclimatic set, the aggregated microclimatic set and the microclimatic set at the
193 native resolution), thus generating three sets of habitat suitability maps for each study species.
194 Background data were generated by sampling an equal amount of background points as occurrence
195 points (i.e., so that species prevalence equals 50%) based on a 2D kernel-density estimate of the
196 occurrence point (Venables & Ripley, 2002), meaning that the spatial density of the background points
197 is proportional to the spatial density of occurrence points for a given species, thereby accounting for
198 spatial bias in the occurrence points (Lake et al., 2020).

199 Although widely-used in scientific research, MaxEnt could suffer from issues like spatial bias
200 and bad model performance due to overfitting (Radosavljevic & Anderson, 2014). To deal with the
201 problem of spatial bias, we conducted spatially independent evaluations in ENMeval2.0 (Kass et al.,
202 2021; Muscarella et al., 2014) using block cross-validation and allocating 80% of our occurrence points
203 to this cross-validation procedure (20% is kept for independent evaluation). Furthermore, model
204 performance was improved by tuning the model settings in ENMeval2.0 rather than working with the
205 default settings of MaxEnt (Supplementary Methods S3). Here, we ensured that feature classes and
206 regularization multipliers were tuned to limit overfitting and increase model performance by using an
207 independent subset of the data (i.e., 20%) not involved in the block cross-validation procedure.

208 **Model performance & sensitivity**

209 In order to customize the settings for the feature classes and the regularization multipliers, a total of
210 24 different models were run for every single species. The Akaike Information Criterion (AIC) for small
211 sample sizes (20 % of occurrence points) was used to select the best candidate models (Burnham &
212 Anderson, 2004). Next, model performance was assessed using the Continuous Boyce Index (CBI),
213 instead of the commonly-used area under the receiver-operating characteristic curve (AUC). The latter
214 has recently been shown to be biased in presence-only models and should therefore be avoided

215 (Jiménez & Soberón, 2020). The CBI is a threshold-independent metric that represents the relationship
216 between predicted habitat suitability and the distribution of occurrence records (Hirzel et al., 2006).
217 Additionally, we calculated the sensitivity enabling us to quantify how good our model is able at
218 distinguishing true positives from false negatives. Both were calculated based on the independent
219 20% subset of the data.

220 Finally, we used Bayesian regression models (BRMs) in order to assess differences in model
221 performance and sensitivity between SDMs constructed using the three different sources of climate
222 data (Supplementary Methods S4). We opted for BRMs as they are able to account for data
223 dependencies (i.e., values clustered within species), unequal variances among groups and skewed
224 distributions. When the highest posterior density intervals ($\alpha = 0.05$) of the contrasts, calculated using
225 the *emmeans* package (Lenth, 2021), did not overlap with zero, contrasts are considered 'significant'.

226 **Model predictions**

227 Habitat suitability was predicted for each species and for each of the three sets of bioclimatic
228 temperature variables (macroclimatic, aggregated microclimatic and microclimatic) for the 2000-2020
229 period. Furthermore, we transformed the logistic maps (i.e., probability values for habitat suitability)
230 to binary (presence-absence) maps using the 10% training presence as a threshold, meaning that the
231 suitable area contains 90% of the original occurrence records (Benito et al., 2013).

232 To compare between model predictions from SDMs constructed with different climate
233 sources and resolutions, we calculated both the potential suitable area and the potential latitudinal
234 range of each species. To make a valid comparison between the three climate types, we disaggregated
235 the binary maps derived from macroclimatic and aggregated data ($1 \times 1 \text{ km}^2$) to the finer resolution
236 ($25 \times 25 \text{ m}^2$), and subsequently masked out all non-forest pixels. First, the potential suitable area (km^2),
237 for each modelled species, was calculated as the sum of all forest pixels classified as potentially
238 suitable under the binary maps. Second, the northern and southern latitudinal limit of the predicted
239 distributional ranges were defined as the 95% and 5% quantile in latitudinal position, respectively, of
240 all pixels classified as potentially suitable. Next, we quantified species thermal response curves for
241 mean annual temperature (BIO1), maximum temperature of the warmest month (BIO5) and minimum
242 temperature of the coldest month (BIO6) by extracting the climatic conditions over the entire
243 potentially suitable area. To optimize computation power, we randomly sampled 1,000,000 pixels
244 over the potentially suitable area for microclimate-based maps. For each variable, we derived the cold
245 limit (Q05), the optimum (mode), the warm limit (Q95), and the niche width (Q95 – Q05). Analogous
246 to the model performance calculations, we used BRMs with the same settings to assess differences in

247 model predictions between the SDMs based on the three types of climate data (Table S2). Values of
248 bioclimatic variables were standardized before the analysis to aid model convergence.

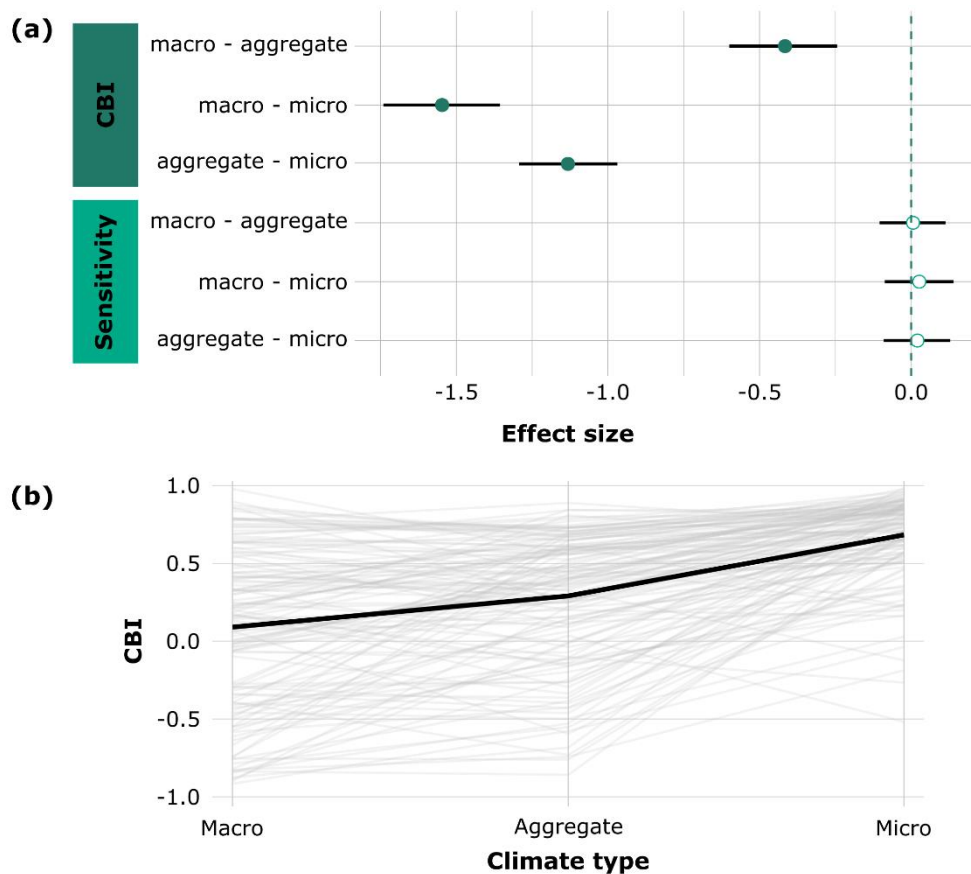
249 Finally, we analyzed whether species are constrained to specific (relative) temperature
250 conditions (i.e., here defined as microrefugia) at their northern and southern latitudinal limits, as this
251 is important for biodiversity conservation. For the northern and southern latitudinal limit, we
252 extracted the 5% most southern and northern occurrence records, respectively. Using paired two-
253 sided t-tests ($\alpha = 0.05$), we compared the local temperature conditions of these occurrence points to
254 the mean surrounding microclimatic conditions over a range of circular buffers (i.e., 100 m, 500 m,
255 1000 m, 2500 m, 5000 m; Figure S2) around each occurrence record. A significant t-test implied a
256 significant difference in local temperatures at the presence locations as compared with the
257 surrounding area, suggesting that occurrences were restricted to microrefugia.

258 All calculations were performed in R version 4.1.1 (R Core Team, 2021). The Tier-2 Genius
259 cluster from the high-performance computing facilities of Flanders was used to make the predictions.
260 In order to improve reproducibility, we followed the ODMAP (Overview, Data, Model, Assessment and
261 Prediction; Zurell et al., 2020) protocol to report on the SDMs in this study (Table S3).

262 **RESULTS**

263 **Model performance & sensitivity**

264 We found significant differences ($\alpha = 0.05$) in model performance between models constructed with:
 265 (i) macroclimatic (mean CBI = 0.09; se = 0.04) and microclimatic (mean CBI = 0.67; se = 0.02) data; (ii)
 266 macroclimatic and microclimatic data but aggregated at a spatial resolution matching macroclimate
 267 data (mean CBI = 0.28; se = 0.04); and (iii) aggregated microclimatic and microclimatic data at the
 268 native resolution (Figure 2a). For 92% of the species, fine-grained microclimate data systematically
 269 improved model performance (Figure 2b). Here, 39% of macroclimate-based SDMs are characterized
 270 by CBI values smaller than zero, meaning that these models perform worse than random. On the other
 271 hand, CBI values are positive for almost all (96%) microclimate-based SDMs. Furthermore, there were
 272 no significant differences between any of the groups regarding the sensitivity of the models.

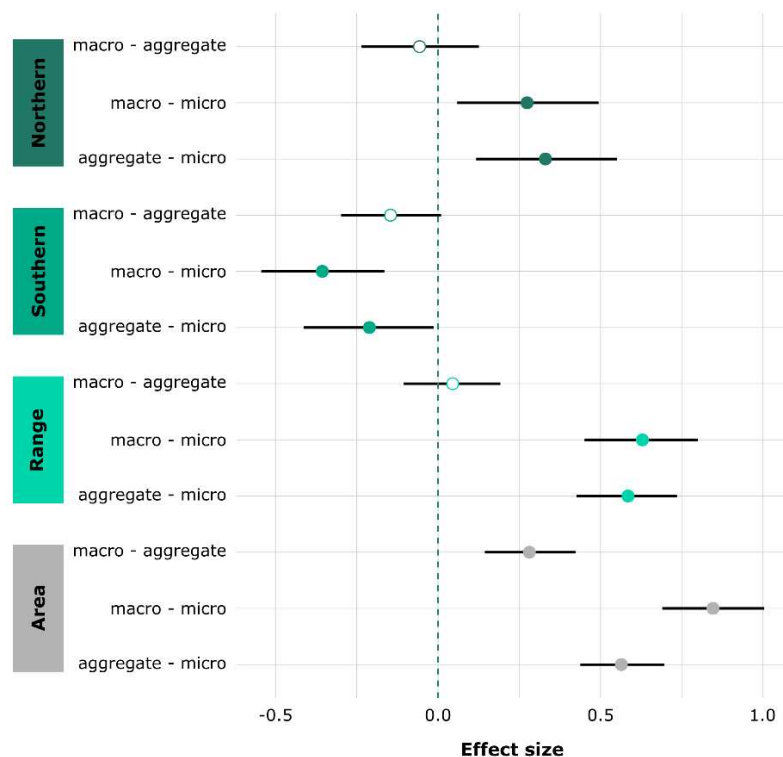


273

274 *Figure 2: (a) Pairwise comparison of model performance (quantified as the Continuous Boyce Index, CBI) and*
 275 *sensitivity between SDMs built with macroclimatic, aggregated microclimatic and microclimatic data. A positive*
 276 *effect size of the comparison reflects a higher model performance and sensitivity in SDMs built with the first*
 277 *group of climate data compared to the second group of climate data. Negative effect sizes reflect the opposite*
 278 *result. Points and associated black error bars correspond to posterior means and 95% highest posterior density*
 279 *intervals of the differences (of the scaled CBI and sensitivity). Significant differences are indicated by solid dots*
 280 *whereas non-significant differences are indicated by transparent dots; (b) The performance of each SDM per*
 281 *species (grey lines) over the three types of climate data (i.e., macroclimatic data, aggregated microclimatic data*
 282 *and microclimatic data). The thick black line shows the average CBI value over each of the three climate types.*

283 **Potential suitable area & latitudinal range**

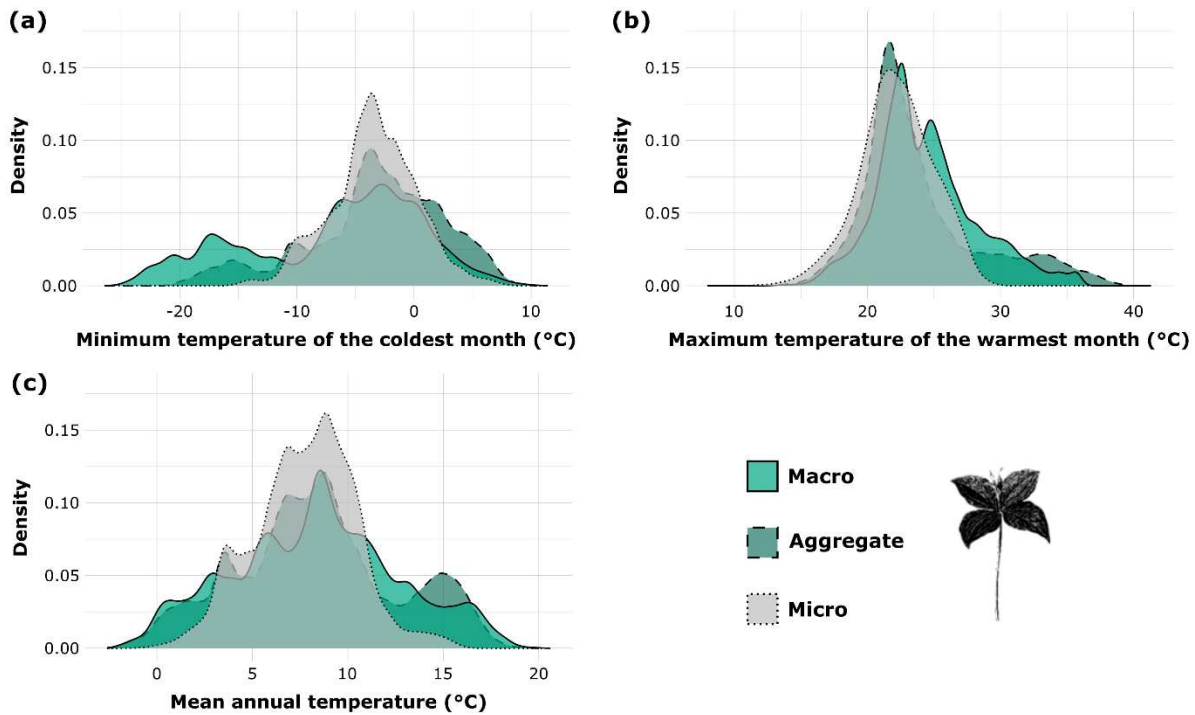
284 The binary distribution maps showed clear differences in the potential suitable area and the potential
 285 latitudinal range covered by each species between models calibrated with macroclimatic data and
 286 models calibrated with microclimatic data at the native spatial resolution of $25 \times 25 \text{ m}^2$ (e.g., *Paris*
 287 *quadrifolia*; Figure S3). Bayesian regression models confirm these visual interpretations for all
 288 modelled species (Figure 3). Relative to microclimate-based SDMs at the native spatial resolution,
 289 both the northern and southern limit of the species' latitudinal ranges are significantly overestimated
 290 when using either macroclimate-based SDMs or the aggregated version of microclimate-based SDMs.
 291 Consequently, species' potential latitudinal ranges are significantly narrower when using SDMs
 292 calibrated with microclimatic data (mean = 2,261 km; se = 42 km) in comparison with SDMs calibrated
 293 with aggregated microclimatic data (mean = 2,580 km; se = 43 km) or macroclimatic data (mean =
 294 2,620 km; se = 49 km). Analogous, a species' potential suitable area is significantly smaller when using
 295 SDMs calibrated with microclimatic data (mean = 911,845 km^2 ; se = 30,383 km^2) in comparison with
 296 SDMs calibrated with aggregated microclimatic data (mean = 1,148,763 km^2 ; se = 33,527 km^2) or
 297 macroclimatic data (mean = 1,268,189 km^2 ; se = 38,274 km^2).



298
 299 *Figure 3: Pairwise comparison of the northern edge, southern edge, latitudinal range and potential suitable area,*
 300 *respectively between SDMs build with macroclimatic, aggregated microclimatic and microclimatic data. A*
 301 *positive effect size of the comparison reflects more northern latitudinal limits (at the northern and/or southern*
 302 *edge), higher latitudinal ranges and more potentially suitable area in SDMs built with the first group of climate*
 303 *data compared to the second group of climate data. Negative effect sizes reflect the opposite result. Points and*
 304 *associated black error bars correspond to posterior means and 95% highest posterior density intervals of the*
 305 *differences (of the standardized variables). Significant differences are indicated by solid dots whereas non-*
 306 *significant differences are indicated by transparent dots.*

307 **Species response curves**

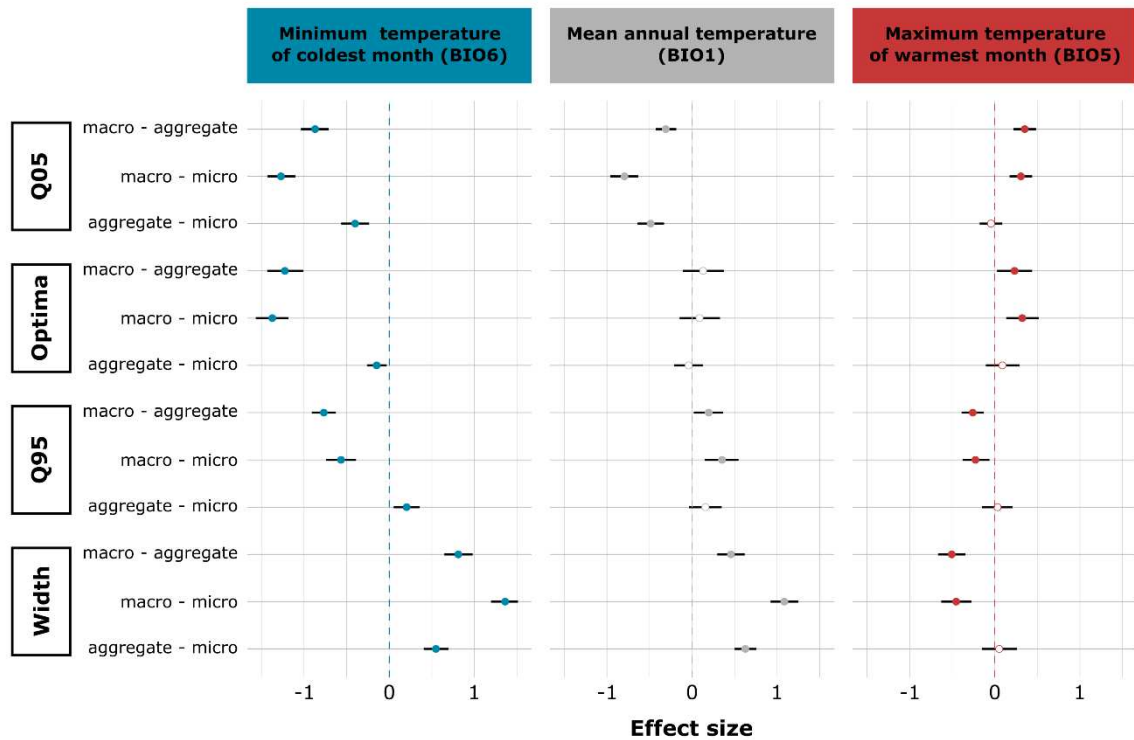
308 A first visual assessment of the response curves showed that microclimate-based response curves of
309 minimum temperature of the coldest month, mean annual temperature and maximum temperature
310 of the warmest month have different optima, and narrower niches compared to macroclimate-based
311 response curves (e.g., *Paris quadrifolia*; Figure 4).



312

313 *Figure 4: Species response curves for (a) minimum temperature of the coldest month, (b) maximum temperature*
314 *of the warmest month and (c) mean annual temperature for Paris quadrifolia, illustrating the buffering effect*
315 *that forest could exert on the thermal niche of species. Here, minimum temperatures are buffered at the cold*
316 *edge of the response curve, whereas maximum temperatures are buffered at the warm edge of the response*
317 *curve.*

318 Bayesian regression models showed that, for all modelled species, optima significantly differed
319 between SDMs run with microclimate and macroclimate data for minimum and maximum
320 temperatures, with warmer optima in minimum temperature and cooler optima in maximum
321 temperature for microclimate-based SDMs relative to macroclimate based SDMs (Figure 5). However,
322 for mean temperature there were no significant differences in optima between the different climate
323 types. Furthermore, the niche width was narrower in minimum and mean temperatures for
324 microclimate-based SDMs relative to macroclimate based SDMs. Surprisingly, the niche width was
325 significantly wider in maximum temperatures for microclimate-based SDMs relative to macroclimate
326 based SDMs.

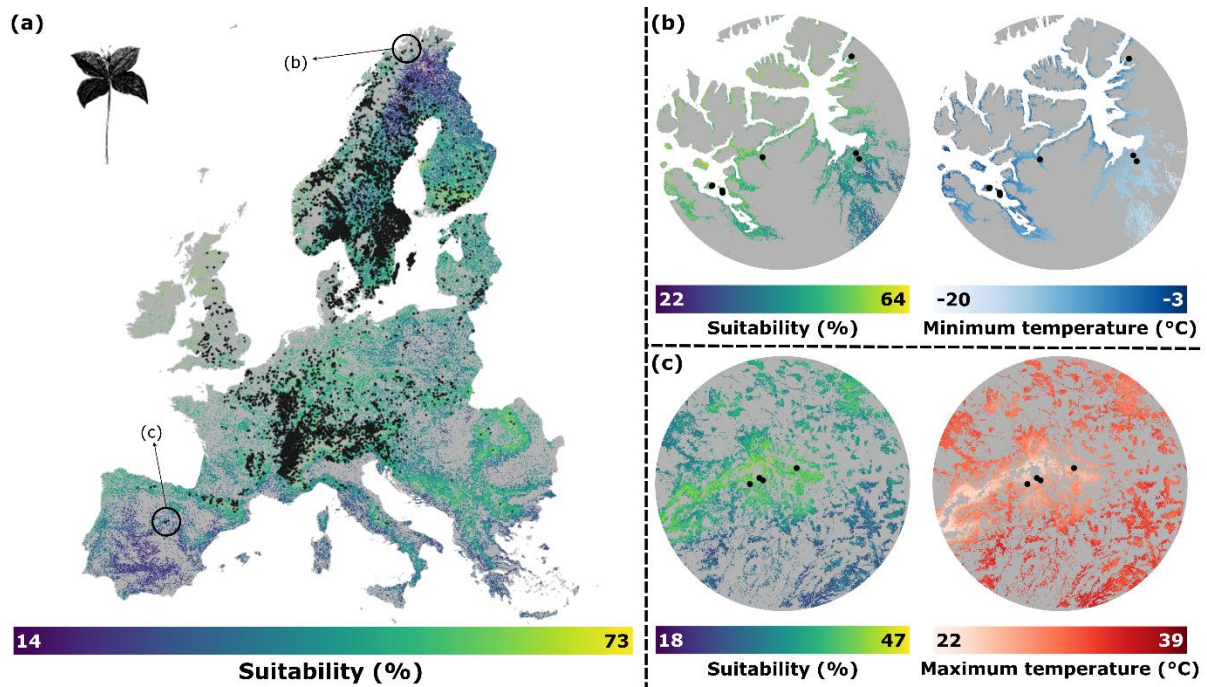


327

328 *Figure 5: Pairwise comparison of the cold edge (Q05), optimum, warm edge (Q95) and niche width, respectively*
 329 *between SDMs build with macroclimatic, aggregated microclimatic and microclimatic data. Each of the*
 330 *comparisons is made for minimum temperature of the coldest month (BIO6), mean annual temperature (BIO1),*
 331 *and maximum temperature of the warmest month (BIO5), respectively. A positive effect size reflects warmer*
 332 *values for the cold edge, optima and warm edge as well as wider niche widths, respectively, in SDMs built with*
 333 *the first group of climate data compared to the second group of climate data. Negative effect sizes reflect the*
 334 *opposite result. Points and associated black error bars correspond to posterior means and 95% highest posterior*
 335 *density intervals of the differences (of the standardized variables). Significant differences are indicated by solid*
 336 *dots whereas non-significant differences are indicated by transparent dots.*

337 **Microrefugia**

338 We found that 66% of all studied species are constrained to local microrefugia at their range limits.
 339 More specifically, 41% of the species occur in warm refugia relative to the surrounding landscape, at
 340 the northern limit of their latitudinal while 49% of the modelled species occur as remnant populations
 341 in cool refugia relative to the surrounding landscape, at the southern limit of their latitudinal range
 342 (e.g., *Paris quadrifolia*; Figure 6).



343

344 *Figure 6: (a) Suitability map for Paris quadrifolia resulting from an SDM built with microclimatic data at 25 × 25*
 345 *m² resolution. The black dots represent the occurrence points extracted from GBIF and used as an input to the*
 346 *SDMs. We see that the species can occur in (b) warm refugia (i.e., higher minimum temperature values in the*
 347 *coldest month of the year) at its northern latitudinal limit and in (c) cool refugia (i.e., lower maximum*
 348 *temperature values in the warmest month of the year) at its southern latitudinal limit. The grey background*
 349 *shows non-forest areas.*

350 **DISCUSSION**

351 Over the last years, microclimate research focused on improving our understanding of the drivers
352 behind the differences between microclimate and macroclimate temperatures (Zellweger et al., 2019)
353 and predicting and mapping microclimate temperatures across space and time (Greiser et al., 2018;
354 Kearney et al., 2020). Although the drivers behind forest microclimates are relatively well understood,
355 testing how microclimate layers perform within ecological applications such as SDMs has been limited,
356 especially so across large (e.g., continental) spatial extents. However, with the recent advent of sub-
357 canopy microclimate layers for European forests at 25 × 25 m² resolution, a new avenue of species
358 distribution modelling can be explored (Haesen et al., 2023). We found substantial differences in the
359 model performance (based on the Continuous Boyce Index), indicating that microclimate-based SDMs
360 significantly outperformed their conventional (i.e., macroclimate) counterparts and that aggregating
361 microclimate data at coarser spatial resolutions leads to significant loss in model performance.
362 Importantly, the use of aggregated microclimate data was still a significant improvement over the use
363 of conventional macroclimate data in SDMs, which is especially interesting when computational
364 capacity is limited. Our results thus agree with previous research reporting an increased performance
365 of microclimate-based SDMs on regional scales (Slavich et al., 2014; Stark & Fridley, 2022). However,
366 this study additionally shows significant alterations of the species response curves to temperatures
367 fitted with microclimatic data at a finer spatial resolution, matching the scale of the studied organisms
368 (i.e., understory plants) more closely. This particular finding represents a major scientific advance with
369 important implications in terms of SDMs' abilities to capture physiological processes that better reflect
370 individual fitness.

371 We found significant differences in the shape of the species response curves obtained from
372 the model predictions using different temperature sources. These outcomes underscore the
373 importance of integrating microclimate data into SDMs, as previously proposed by Lembrechts et al.
374 (2019). The recent increased availability of microclimatic data products at fine spatial resolution that
375 cover large spatial extents has enabled us to uncover the true realized thermal niches and reveal the
376 environmental conditions that actually matter for species living close to the ground surface (such as
377 tree seedlings and herbaceous plants growing in the shade of trees). We demonstrate that species
378 response curves derived from conventional macroclimate-based SDMs are much wider than one
379 would expect given the buffering effect of forests (De Frenne et al., 2019; Harwood et al., 2014).
380 Conventional SDMs might thus capture spurious correlations and fail to encompass the genuine
381 factors constraining species distributions. The optima of the species response curves to maximum and
382 minimum temperatures systematically shifted towards colder and warmer conditions, respectively,
383 when using microclimate-based SDMs at fine spatial resolution, suggesting significant improvements

384 in SDMs' abilities to capture plant individual fitness in the forest understory. The same argument
385 applies to the species' thermal tolerance limits as we found systematic shifts towards warmer
386 conditions for the cold and warm tolerance limits of forest understory plants when using
387 microclimate-based SDMs at fine spatial resolution. The ability of microclimate-informed SDMs to
388 more accurately capture thermal tolerance limits holds important implications for exploring broader
389 macrophysiological thermal response patterns and organismal processes (Sentinella et al., 2020;
390 Sunday et al., 2012). This capability could further advance the research domain, aiding in the enhanced
391 comprehension of plants' thermal safety margins in the face of climate change, which are intricately
392 tied to their survival, productivity, and reproductive capacities (Lancaster & Humphreys, 2020).

393 Wider niches estimated by macroclimate-based SDMs also resulted in an overestimation of
394 the predicted range sizes, thereby confirming our second hypothesis. Indeed, the occurrence of a
395 species' individual within a specific macroclimatic pixel does not guarantee that the species will occur
396 in all other macroclimatic pixels with the same temperature because of considerable variations in
397 microclimate heterogeneity. This is especially important at range edges, where species will be found
398 in macroclimate pixels with above-average microclimate heterogeneity. Indeed, the populations of
399 66% of the studied species at the northern and southern limits of their latitudinal range are confined
400 to warm or cold spots in the landscape, respectively (Figure 6; Figure S2). Microclimate-based SDMs
401 thus allow for better identification of local microrefugia. Current macroclimate-based SDM practices
402 are unable to identify these microrefugia correctly as conventional macroclimate data represent the
403 overarching free-air temperatures rather than the local temperatures as perceived by organisms living
404 inside these microrefugia (Lenoir et al., 2017). Given the importance of microrefugia regarding the
405 accumulation and conservation of biodiversity (Nadeau et al., 2022), forest management practices
406 should be optimized to protect local microclimates and increase the capacity of species and
407 communities to resist to climate change (Hylander et al., 2022).

408 There are various reasons for the increased performance of microclimate-based SDMs, which
409 mainly relate to characteristics of the two primary input sources of each SDM: the occurrence points
410 and predictor variables. First, each occurrence point is subjected to a certain amount of positional
411 error (Wüest et al., 2020). In this study, we exclusively used records with a reported coordinate
412 uncertainty below 25 m. Nevertheless, applying a threshold on the positional error like this may induce
413 a loss of model performance by decreasing the number of occurrence points (Guisan et al., 2007).
414 Thus, it is conventionally recommended to decrease the spatial resolution of the analysis to account
415 for any positional errors in the occurrence points, rather than excluding the less precise records.
416 However, SDMs are sensitive to changes in the spatial resolution (Chauvier et al., 2022). Decreasing
417 spatial resolution inherently induces a loss of information as the data is smoothed (i.e., aggregated),

418 which comes at the cost of model performance as shown by the CBI values from the models built with
419 aggregated microclimatic data. Therefore, recent research strongly recommends to fit SDMs as close
420 as possible to the spatial grain that matches the biology of the focal species (Gábor et al., 2022),
421 meaning that it is recommended to calibrate SDMs with environmental data consistent with the
422 biological scale of the system or organism under study (Randin et al., 2009). For instance, when
423 modelling sessile species (i.e., species with limited mobility) or organisms in ecosystems with high
424 environmental heterogeneity, higher-resolution predictors are essential to more precisely capture the
425 intricacies of their niches (Norberg et al., 2019). For example, sessile species are more prone to
426 microclimate limitations due to their inability to actively relocate, rendering them highly sensitive to
427 variability in local environmental conditions and more likely to be spatially limited to habitats with a
428 particular microclimate. As a result, we anticipate that the findings of this study may not be readily
429 transferable when studying mobile species (such as birds or mammals) or uniform environments.

430 Although promising, microclimate-based SDMs inherently face challenges beyond just
431 microclimate considerations. Analogous to other correlative climate-based SDMs, they are likely to
432 fail for many reasons unrelated to the accuracy and resolution of the climate data. For example, SDMs
433 often do not consider demographic processes and biotic interactions that mediate population
434 responses (Sanczuk et al., 2023). However, the SDM toolbox has been extended to accommodate
435 these shortcomings. For instance, range dynamic models explicitly consider demographic processes
436 such as dispersal and population dynamics (Zurell et al., 2016) and joint SDMs infer species
437 interactions from co-occurrence data (Ovaskainen & Abrego, 2020). Genomics-informed SDMs aiming
438 at including adaptability and demographic processes also offer interesting research avenues (Hudson
439 et al., 2021). Additionally, many SDMs do not include the fine-grained spatial heterogeneity of soil
440 conditions that may occur across few meters and which matter for species distributions (Beauregard
441 & de Blois, 2014; Roe et al., 2022). Disregarding the edaphic dimension in SDMs may lead to
442 overestimating the species' potential distribution as well as underestimating its spatial fragmentation
443 with important implications under anthropogenic climate change (Bertrand et al., 2012).

444 Gridded microclimatic data at a resolution of $25 \times 25 \text{ m}^2$ are currently restricted to European
445 forests, which limits this study to 140 forest specialist plant species that exclusively live in forests
446 throughout their range. Herbaceous plant species living in open habitats, such as grasslands or
447 heathlands, are not included, as gridded microclimate data with the necessary spatial resolution is not
448 currently available for these environments at continental scale. The main reason for this is that
449 temperature sensors in open ecosystems are highly exposed to direct solar radiation, leading to
450 significant errors in the measurements recorded by the microclimate loggers (Maclean et al., 2021).
451 Consequently, the development of accurate microclimatic grids for these habitats is hindered.

452 Alternatively, mechanistic models that provided fine-grained gridded data products over large spatial
453 extents could also be used, but they are still missing because of computational challenges (Maclean,
454 2020). Nevertheless, accurate microclimate data over large spatial extents in open systems are
455 urgently needed to assess the transferability of the results from this study to a wider range of species.
456 Finally, while current microclimate products allow improved predictions of current species
457 distributions, microclimatic data predicted under future shared socioeconomic pathways (SSPs) are
458 needed to assess the impact of microclimate change on species ranges or the composition of species
459 communities (Lembrechts, 2023). However, forests are dynamic systems and their structural
460 characteristics that influence the forest microclimate cannot be assumed to remain constant over
461 time, making the development of such products challenging (De Lombaerde et al., 2022; Lenoir et al.,
462 2017). In a warming world, disturbances affecting forest canopies (e.g., drought, pests, storms) will
463 become more frequent and pronounced, drastically affecting the sub-canopy microclimate drastically
464 (Kopáček et al., 2020; Thom et al., 2020) . Given that many forest specialist species have slow dispersal
465 rates, often only several meters per year (Hermy et al., 1999; Svenning et al., 2008), accurately
466 evaluating their distribution ranges becomes crucial. It is very unlikely that these species will be able
467 to keep pace with contemporary macroclimate warming, wherein climate zones are shifting several
468 kilometres each year along the latitudinal gradient (Burrows et al., 2011). In this regard, microclimate-
469 based SDMs may allow us to accurately assess the velocity of microclimate warming experienced by
470 organisms in their immediate habitats and identify the locations where species may become impacted
471 due to climate change. While not explored in this study, this approach could potentially reveal that
472 microclimate heterogeneity mitigates the impact of climate change (Maclean & Early, 2023), and
473 therefore presents opportunities and obvious priorities for area-based conservation.

474 **CONCLUSIONS**

475 To summarize, our study highlights the significant benefits of including microclimatic data in species
476 distribution models for forest plant species. By using microclimate-based SDMs, we were able to
477 uncover the hidden niche of forest plants, providing insights into their tolerance limits in response to
478 climate warming. This is in contrast to macroclimatic data, which estimated broader niches and could
479 not identify warm and cold refugia at the range edges of species distributions. Microclimate-based
480 SDMs are therefore essential for biodiversity conservation in the face of climate change, by providing
481 insights to optimize management actions and prioritize conservation efforts, particularly given the
482 growing policy and management focus on conservation of refugia worldwide.

483 **ACKNOWLEDGEMENTS**

484 This work was funded by Internal Funds of KU Leuven, an FWO Research Network Grant to SoilTemp
485 (W001919N) and the COST Action CA18201 – ConservePlants. SH was supported by a FLOF fellowship
486 (project nr. 3E190655) of the KU Leuven. JL received funding from: (i) the Agence Nationale de la
487 Recherche (ANR) (project IMPRINT; <https://microclimat.cnrs.fr>; grant nr. ANR-19-CE32-0005-01); (ii)
488 the Centre National de la Recherche Scientifique (CNRS) through the MITI interdisciplinary programs
489 (Défi INFINITI 2018: MORFO); (iii) and the Structure Fédérative de Recherche (SFR) Condorcet (FR CNRS
490 3417: CREUSE). JLL is funded by the Research Foundation Flanders (12P1819N) and by the ASICS
491 project (ANR-20-EBI5-0004, BiodivERsA, BiodivClim call 2019–2020). The study was also supported by
492 the Czech Science Foundation (project GACR 20-28119S) and the Czech Academy of Sciences (project
493 RVO 67985939). ChatGPT was used to improve English grammar and flow of the text.

494 The computational resources and services used in this work were provided by the VSC (Flemish
495 Supercomputer Center), funded by the Research Foundation Flanders (FWO) and the Flemish
496 Government – department EWI.

497 **REFERENCES**

- 498 Abatzoglou, J. T., Dobrowski, S. Z., Parks, S. A., & Hegewisch, K. C. (2018). TerraClimate, a high-
499 resolution global dataset of monthly climate and climatic water balance from 1958–2015.
500 *Scientific Data*, 5(1), 170191. <https://doi.org/10.1038/sdata.2017.191>
- 501 Beauregard, F., & de Blois, S. (2014). Beyond a Climate-Centric View of Plant Distribution: Edaphic
502 Variables Add Value to Distribution Models. *PLoS ONE*, 9(3), e92642.
503 <https://doi.org/10.1371/journal.pone.0092642>
- 504 Benito, B. M., Cayuela, L., & Albuquerque, F. S. (2013). The impact of modelling choices in the
505 predictive performance of richness maps derived from species-distribution models: guidelines to
506 build better diversity models. *Methods in Ecology and Evolution*, 4(4), 327–335.
507 <https://doi.org/10.1111/2041-210x.12022>
- 508 Bertrand, R., Perez, V., & Gégout, J.-C. (2012). Disregarding the edaphic dimension in species
509 distribution models leads to the omission of crucial spatial information under climate change:
510 the case of *Quercus pubescens* in France. *Global Change Biology*, 18(8), 2648–2660.
511 <https://doi.org/10.1111/j.1365-2486.2012.02679.x>

512 Booth, T. H. (2022). Checking bioclimatic variables that combine temperature and precipitation data
513 before their use in species distribution models. *Austral Ecology*, 47(7), 1506–1514.
514 <https://doi.org/10.1111/aec.13234>

515 Booth, T. H., Nix, H. A., Busby, J. R., & Hutchinson, M. F. (2014). bioclim: the first species distribution
516 modelling package, its early applications and relevance to most current MaxEnt studies. *Diversity
517 and Distributions*, 20(1), 1–9. <https://doi.org/10.1111/ddi.12144>

518 Burnham, K. P., & Anderson, D. R. (2004). Multimodel Inference. *Sociological Methods & Research*,
519 33(2), 261–304. <https://doi.org/10.1177/0049124104268644>

520 Burrows, M. T., Schoeman, D. S., Buckley, L. B., Moore, P., Poloczanska, E. S., Brander, K. M., Brown,
521 C., Bruno, J. F., Duarte, C. M., Halpern, B. S., Holding, J., Kappel, C. V., Kiessling, W., O'Connor, M.
522 I., Pandolfi, J. M., Parmesan, C., Schwing, F. B., Sydeman, W. J., & Richardson, A. J. (2011). The
523 Pace of Shifting Climate in Marine and Terrestrial Ecosystems. *Science*, 334(6056), 652–655.
524 <https://doi.org/10.1126/science.1210288>

525 Caron, M. M., Zellweger, F., Verheyen, K., Baeten, L., Hédli, R., Bernhardt-Römermann, M., Berki, I.,
526 Brunet, J., Decocq, G., Díaz, S., Dirnböck, T., Durak, T., Heinken, T., Jaroszewicz, B., Kopecký, M.,
527 Lenoir, J., Macek, M., Malicki, M., Máliš, F., ... De Frenne, P. (2021). Thermal differences between
528 juveniles and adults increased over time in European forest trees. *Journal of Ecology*, 109(11),
529 3944–3957. <https://doi.org/10.1111/1365-2745.13773>

530 Chauvier, Y., Descombes, P., Guéguen, M., Boulangeat, L., Thuiller, W., & Zimmermann, N. E. (2022).
531 Resolution in species distribution models shapes spatial patterns of plant multifaceted diversity.
532 *Ecography*, 2022(10). <https://doi.org/10.1111/ecog.05973>

533 Cheng, Y., Tjaden, N. B., Jaeschke, A., Thomas, S. M., & Beierkuhnlein, C. (2021). Using centroids of
534 spatial units in ecological niche modelling: Effects on model performance in the context of
535 environmental data grain size. *Global Ecology and Biogeography*, 30(3), 611–621.
536 <https://doi.org/10.1111/geb.13240>

537 De Frenne, P., Zellweger, F., Rodríguez-Sánchez, F., Scheffers, B. R., Hylander, K., Luoto, M., Vellend,
538 M., Verheyen, K., & Lenoir, J. (2019). Global buffering of temperatures under forest canopies.
539 *Nature Ecology & Evolution*, 3(5), 744–749. <https://doi.org/10.1038/s41559-019-0842-1>

540 De Lombaerde, E., Vangansbeke, P., Lenoir, J., Van Meerbeek, K., Lembrechts, J., Rodríguez-Sánchez,
541 F., Luoto, M., Scheffers, B., Haesen, S., Aalto, J., Christiansen, D. M., De Pauw, K., Depauw, L.,
542 Govaert, S., Greiser, C., Hampe, A., Hylander, K., Klinges, D., Koelemeijer, I., ... De Frenne, P.

543 (2022). Maintaining forest cover to enhance temperature buffering under future climate change.
544 *Science of The Total Environment*, 810, 151338.
545 <https://doi.org/10.1016/j.scitotenv.2021.151338>

546 Dormann, C. F., Elith, J., Bacher, S., Buchmann, C., Carl, G., Carré, G., Marquéz, J. R. G., Gruber, B.,
547 Lafourcade, B., Leitão, P. J., Münkemüller, T., McClean, C., Osborne, P. E., Reineking, B., Schröder,
548 B., Skidmore, A. K., Zurell, D., & Lautenbach, S. (2013). Collinearity: a review of methods to deal
549 with it and a simulation study evaluating their performance. *Ecography*, 36(1), 27–46.
550 <https://doi.org/10.1111/j.1600-0587.2012.07348.x>

551 Elith, J., & Leathwick, J. R. (2009). Species Distribution Models: Ecological Explanation and Prediction
552 Across Space and Time. *Annual Review of Ecology, Evolution, and Systematics*, 40(1), 677–697.
553 <https://doi.org/10.1146/annurev.ecolsys.110308.120159>

554 Fick, S. E., & Hijmans, R. J. (2017). WorldClim 2: new 1-km spatial resolution climate surfaces for global
555 land areas. *International Journal of Climatology*, 37(12), 4302–4315.
556 <https://doi.org/10.1002/joc.5086>

557 Fourcade, Y., Besnard, A. G., & Secondi, J. (2018). Paintings predict the distribution of species, or the
558 challenge of selecting environmental predictors and evaluation statistics. *Global Ecology and*
559 *Biogeography*, 27(2), 245–256. <https://doi.org/10.1111/geb.12684>

560 Gábor, L., Jetz, W., Lu, M., Rocchini, D., Cord, A., Malavasi, M., Zarzo-Arias, A., Barták, V., & Moudrý,
561 V. (2022). Positional errors in species distribution modelling are not overcome by the coarser
562 grains of analysis. *Methods in Ecology and Evolution*, 13(10), 2289–2302.
563 <https://doi.org/10.1111/2041-210X.13956>

564 Geiger, R. (1950). *The climate near the ground*. Cambridge, Mass.: Harvard University Press. 482p.
565 pages.

566 Greiser, C., Meineri, E., Luoto, M., Ehrén, J., & Hylander, K. (2018). Monthly microclimate models in a
567 managed boreal forest landscape. *Agricultural and Forest Meteorology*, 250–251, 147–158.
568 <https://doi.org/10.1016/j.agrformet.2017.12.252>

569 Guisan, A., Graham, C. H., Elith, J., & Huettmann, F. (2007). Sensitivity of predictive species distribution
570 models to change in grain size. *Diversity and Distributions*, 13(3), 332–340.
571 <https://doi.org/10.1111/j.1472-4642.2007.00342.x>

572 Haesen, S., Lembrechts, J. J., De Frenne, P., Lenoir, J., Aalto, J., Ashcroft, M. B., Kopecký, M., Luoto, M.,
573 Maclean, I., Nijs, I., Niittynen, P., Hoogen, J., Arriga, N., Brůna, J., Buchmann, N., Čiliak, M.,

574 Collalti, A., De Lombaerde, E., Descombes, P., ... Van Meerbeek, K. (2021). ForestTemp – Sub-
575 canopy microclimate temperatures of European forests. *Global Change Biology*, 27(23), 6307–
576 6319. <https://doi.org/10.1111/gcb.15892>

577 Haesen, S., Lembrechts, J. J., De Frenne, P., Lenoir, J., Aalto, J., Ashcroft, M. B., Kopecký, M., Luoto, M.,
578 Maclean, I., Nijs, I., Niittynen, P., van den Hoogen, J., Arriga, N., Brůna, J., Buchmann, N., Čiliak,
579 M., Collalti, A., De Lombaerde, E., Descombes, P., ... Van Meerbeek, K. (2023). ForestClim —
580 Bioclimatic variables for microclimate temperatures of European forests. *Global Change Biology*,
581 29(11), 2886–2892. <https://doi.org/10.1111/gcb.16678>

582 Hageer, Y., Esperón-Rodríguez, M., Baumgartner, J. B., & Beaumont, L. J. (2017). Climate, soil or both?
583 Which variables are better predictors of the distributions of Australian shrub species? *PeerJ*, 5(6),
584 e3446. <https://doi.org/10.7717/peerj.3446>

585 Harwood, T. D., Mokany, K., & Paini, D. R. (2014). Microclimate is integral to the modeling of plant
586 responses to macroclimate. *Proceedings of the National Academy of Sciences*, 111(13).
587 <https://doi.org/10.1073/pnas.1400069111>

588 Heinken, T., Diekmann, M., Liira, J., Orczewska, A., Schmidt, M., Brunet, J., Chytrý, M., Chabrierie, O.,
589 Decocq, G., De Frenne, P., Dřevojan, P., Dzwonko, Z., Ewald, J., Feilberg, J., Graae, B. J., Grytnes,
590 J., Hermy, M., Kriebitzsch, W., Laiviņš, M., ... Vanneste, T. (2022). The European Forest Plant
591 Species List (EuForPlant): Concept and applications. *Journal of Vegetation Science*, 33(3).
592 <https://doi.org/10.1111/jvs.13132>

593 Hermy, M., Honnay, O., Firbank, L., Grashof-Bokdam, C., & Lawesson, J. E. (1999). An ecological
594 comparison between ancient and other forest plant species of Europe, and the implications for
595 forest conservation. *Biological Conservation*, 91(1), 9–22. [https://doi.org/10.1016/S0006-
596 3207\(99\)00045-2](https://doi.org/10.1016/S0006-3207(99)00045-2)

597 Hirzel, A. H., Le Lay, G., Helfer, V., Randin, C., & Guisan, A. (2006). Evaluating the ability of habitat
598 suitability models to predict species presences. *Ecological Modelling*, 199(2), 142–152.
599 <https://doi.org/10.1016/j.ecolmodel.2006.05.017>

600 Hudson, J., Castilla, J. C., Teske, P. R., Beheregaray, L. B., Haigh, I. D., McQuaid, C. D., & Rius, M. (2021).
601 Genomics-informed models reveal extensive stretches of coastline under threat by an
602 ecologically dominant invasive species. *Proceedings of the National Academy of Sciences*,
603 118(23), e2022169118. <https://doi.org/10.1073/pnas.2022169118>

604 Hylander, K., Greiser, C., Christiansen, D. M., & Koelemeijer, I. A. (2022). Climate adaptation of
605 biodiversity conservation in managed forest landscapes. *Conservation Biology*, *36*(3), e13847.
606 <https://doi.org/10.1111/cobi.13847>

607 Jarraud, M. (2008). *Guide to meteorological instruments and methods of observation (WMO-No. 8)*.

608 Jiménez, L., & Soberón, J. (2020). Leaving the area under the receiving operating characteristic curve
609 behind: An evaluation method for species distribution modelling applications based on presence-
610 only data. *Methods in Ecology and Evolution*, *11*(12), 1571–1586. [https://doi.org/10.1111/2041-
611 210X.13479](https://doi.org/10.1111/2041-210X.13479)

612 Karger, D. N., Conrad, O., Böhrer, J., Kawohl, T., Kreft, H., Soria-Auza, R. W., Zimmermann, N. E., Linder,
613 H. P., & Kessler, M. (2017). Climatologies at high resolution for the earth's land surface areas.
614 *Scientific Data*, *4*(1), 170122. <https://doi.org/10.1038/sdata.2017.122>

615 Kass, J. M., Muscarella, R., Galante, P. J., Bohl, C. L., Pinilla-Buitrago, G. E., Boria, R. A., Soley-Guardia,
616 M., & Anderson, R. P. (2021). ENMeval 2.0: Redesigned for customizable and reproducible
617 modeling of species' niches and distributions. *Methods in Ecology and Evolution*, *12*(9), 1602–
618 1608. <https://doi.org/10.1111/2041-210X.13628>

619 Kearney, M. R., Gillingham, P. K., Bramer, I., Duffy, J. P., & Maclean, I. M. D. (2020). A method for
620 computing hourly, historical, terrain-corrected microclimate anywhere on earth. *Methods in
621 Ecology and Evolution*, *11*(1), 38–43. <https://doi.org/10.1111/2041-210X.13330>

622 Kopáček, J., Bače, R., Hejzlar, J., Kaňa, J., Kučera, T., Matějka, K., Porcal, P., & Turek, J. (2020). Changes
623 in microclimate and hydrology in an unmanaged mountain forest catchment after insect-induced
624 tree dieback. *Science of The Total Environment*, *720*, 137518.
625 <https://doi.org/10.1016/j.scitotenv.2020.137518>

626 Körner, C., & Hiltbrunner, E. (2018). The 90 ways to describe plant temperature. *Perspectives in Plant
627 Ecology, Evolution and Systematics*, *30*, 16–21. <https://doi.org/10.1016/j.ppees.2017.04.004>

628 Lake, T. A., Briscoe Runquist, R. D., & Moeller, D. A. (2020). Predicting range expansion of invasive
629 species: Pitfalls and best practices for obtaining biologically realistic projections. *Diversity and
630 Distributions*, *26*(12), 1767–1779. <https://doi.org/10.1111/ddi.13161>

631 Lancaster, L. T., & Humphreys, A. M. (2020). Global variation in the thermal tolerances of plants.
632 *Proceedings of the National Academy of Sciences*, *117*(24), 13580–13587.
633 <https://doi.org/10.1073/pnas.1918162117>

634 Lembrechts, J. J. (2023). Microclimate alters the picture. *Nature Climate Change*, 13(5), 423–424.
635 <https://doi.org/10.1038/s41558-023-01632-5>

636 Lembrechts, J. J., Nijs, I., & Lenoir, J. (2019). Incorporating microclimate into species distribution
637 models. *Ecography*, 42(7), 1267–1279. <https://doi.org/10.1111/ecog.03947>

638 Lenoir, J., Hattab, T., & Pierre, G. (2017). Climatic microrefugia under anthropogenic climate change:
639 implications for species redistribution. *Ecography*, 40(2), 253–266.
640 <https://doi.org/10.1111/ecog.02788>

641 Lenth, R. V. (2021). *emmeans: Estimated Marginal Means, aka Least-Squares Means*.

642 Macek, M., Kopecký, M., & Wild, J. (2019). Maximum air temperature controlled by landscape
643 topography affects plant species composition in temperate forests. *Landscape Ecology*, 34(11),
644 2541–2556. <https://doi.org/10.1007/s10980-019-00903-x>

645 Maclean, I. M. D. (2020). Predicting future climate at high spatial and temporal resolution. *Global*
646 *Change Biology*, 26(2), 1003–1011. <https://doi.org/10.1111/gcb.14876>

647 Maclean, I. M. D., Duffy, J. P., Haesen, S., Govaert, S., De Frenne, P., Vanneste, T., Lenoir, J.,
648 Lembrechts, J. J., Rhodes, M. W., & Van Meerbeek, K. (2021). On the measurement of
649 microclimate. *Methods in Ecology and Evolution*, 12(8), 1397–1410.
650 <https://doi.org/10.1111/2041-210X.13627>

651 Maclean, I. M. D., & Early, R. (2023). Macroclimate data overestimate range shifts of plants in response
652 to climate change. *Nature Climate Change*, 13(5), 484–490. [https://doi.org/10.1038/s41558-](https://doi.org/10.1038/s41558-023-01650-3)
653 [023-01650-3](https://doi.org/10.1038/s41558-023-01650-3)

654 Man, M., Wild, J., Macek, M., & Kopecký, M. (2022). Can high-resolution topography and forest canopy
655 structure substitute microclimate measurements? Bryophytes say no. *Science of The Total*
656 *Environment*, 821, 153377. <https://doi.org/10.1016/j.scitotenv.2022.153377>

657 Muscarella, R., Galante, P. J., Soley-Guardia, M., Boria, R. A., Kass, J. M., Uriarte, M., & Anderson, R. P.
658 (2014). ENMeval: An R package for conducting spatially independent evaluations and estimating
659 optimal model complexity for Maxent ecological niche models. *Methods in Ecology and*
660 *Evolution*, 5(11), 1198–1205. <https://doi.org/10.1111/2041-210X.12261>

661 Nadeau, C. P., Giacomazzo, A., & Urban, M. C. (2022). Cool microrefugia accumulate and conserve
662 biodiversity under climate change. *Global Change Biology*, 28(10), 3222–3235.
663 <https://doi.org/10.1111/gcb.16143>

664 Norberg, A., Abrego, N., Blanchet, F. G., Adler, F. R., Anderson, B. J., Anttila, J., Araújo, M. B., Dallas,
665 T., Dunson, D., Elith, J., Foster, S. D., Fox, R., Franklin, J., Godsoe, W., Guisan, A., O'Hara, B., Hill,
666 N. A., Holt, R. D., Hui, F. K. C., ... Ovaskainen, O. (2019). A comprehensive evaluation of predictive
667 performance of 33 species distribution models at species and community levels. *Ecological*
668 *Monographs*, 89(3), e01370. <https://doi.org/10.1002/ecm.1370>

669 Ovaskainen, O., & Abrego, N. (2020). *Joint Species Distribution Modelling*. Cambridge University Press.
670 <https://doi.org/10.1017/9781108591720>

671 Phillips, S. J., Anderson, R. P., Dudík, M., Schapire, R. E., & Blair, M. E. (2017). Opening the black box:
672 an open-source release of Maxent. *Ecography*, 40(7), 887–893.
673 <https://doi.org/10.1111/ecog.03049>

674 R Core Team. (2021). *R: A Language and Environment for Statistical Computing*.

675 Radosavljevic, A., & Anderson, R. P. (2014). Making better Maxent models of species distributions:
676 complexity, overfitting and evaluation. *Journal of Biogeography*, 41(4), 629–643.
677 <https://doi.org/10.1111/jbi.12227>

678 Randin, C. F., Engler, R., Normand, S., Zappa, M., Zimmermann, N. E., Pearman, P. B., Vittoz, P., Thuiller,
679 W., & Guisan, A. (2009). Climate change and plant distribution: local models predict high-
680 elevation persistence. *Global Change Biology*, 15(6), 1557–1569.
681 <https://doi.org/10.1111/j.1365-2486.2008.01766.x>

682 Roe, N. A., Ducey, M. J., Lee, T. D., Fraser, O. L., Colter, R. A., & Hallett, R. A. (2022). Soil chemical
683 variables improve models of understory plant species distributions. *Journal of Biogeography*,
684 49(4), 753–766. <https://doi.org/10.1111/jbi.14344>

685 Sanczuk, P., De Pauw, K., De Lombaerde, E., Luoto, M., Meeussen, C., Govaert, S., Vanneste, T.,
686 Depauw, L., Brunet, J., Cousins, S. A. O., Gasperini, C., Hedwall, P.-O., Iacopetti, G., Lenoir, J., Plue,
687 J., Selvi, F., Spicher, F., Uria-Diez, J., Verheyen, K., ... De Frenne, P. (2023). Microclimate and forest
688 density drive plant population dynamics under climate change. *Nature Climate Change*, 13(8),
689 840–847. <https://doi.org/10.1038/s41558-023-01744-y>

690 Sentinella, A. T., Warton, D. I., Sherwin, W. B., Offord, C. A., & Moles, A. T. (2020). Tropical plants do
691 not have narrower temperature tolerances, but are more at risk from warming because they are
692 close to their upper thermal limits. *Global Ecology and Biogeography*, 29(8), 1387–1398.
693 <https://doi.org/10.1111/geb.13117>

- 694 Slavich, E., Warton, D. I., Ashcroft, M. B., Gollan, J. R., & Ramp, D. (2014). Topoclimate versus
695 macroclimate: how does climate mapping methodology affect species distribution models and
696 climate change projections? *Diversity and Distributions*, 20(8), 952–963.
697 <https://doi.org/10.1111/ddi.12216>
- 698 Stark, J. R., & Fridley, J. D. (2022). Microclimate-based species distribution models in complex forested
699 terrain indicate widespread cryptic refugia under climate change. *Global Ecology and*
700 *Biogeography*, 31(3), 562–575. <https://doi.org/10.1111/geb.13447>
- 701 Sunday, J. M., Bates, A. E., & Dulvy, N. K. (2012). Thermal tolerance and the global redistribution
702 of animals. *Nature Climate Change*, 2(9), 686–690. <https://doi.org/10.1038/nclimate1539>
- 703 Svenning, J.-C., Normand, S., & Skov, F. (2008). Postglacial dispersal limitation of widespread forest
704 plant species in nemoral Europe. *Ecography*, 31(3), 316–326. [https://doi.org/10.1111/j.0906-](https://doi.org/10.1111/j.0906-7590.2008.05206.x)
705 [7590.2008.05206.x](https://doi.org/10.1111/j.0906-7590.2008.05206.x)
- 706 Thom, D., Sommerfeld, A., Sebald, J., Hagge, J., Müller, J., & Seidl, R. (2020). Effects of disturbance
707 patterns and deadwood on the microclimate in European beech forests. *Agricultural and Forest*
708 *Meteorology*, 291, 108066. <https://doi.org/10.1016/j.agrformet.2020.108066>
- 709 van Proosdij, A. S. J., Sosef, M. S. M., Wieringa, J. J., & Raes, N. (2016). Minimum required number of
710 specimen records to develop accurate species distribution models. *Ecography*, 39(6), 542–552.
711 <https://doi.org/10.1111/ecog.01509>
- 712 Venables, W. N., & Ripley, B. D. (2002). *Modern Applied Statistics with S, Fourth edition*. Springer, New
713 York.
- 714 Wüest, R. O., Zimmermann, N. E., Zurell, D., Alexander, J. M., Fritz, S. A., Hof, C., Kreft, H., Normand,
715 S., Cabral, J. S., Szekely, E., Thuiller, W., Wikelski, M., & Karger, D. N. (2020). Macroecology in the
716 age of Big Data – Where to go from here? *Journal of Biogeography*, 47(1), 1–12.
717 <https://doi.org/10.1111/jbi.13633>
- 718 Zellweger, F., Coomes, D., Lenoir, J., Depauw, L., Maes, S. L., Wulf, M., Kirby, K. J., Brunet, J., Kopecký,
719 M., Máliš, F., Schmidt, W., Heinrichs, S., den Ouden, J., Jaroszewicz, B., Buyse, G., Spicher, F.,
720 Verheyen, K., & De Frenne, P. (2019). Seasonal drivers of understorey temperature buffering in
721 temperate deciduous forests across Europe. *Global Ecology and Biogeography*, 28(12), 1774–
722 1786. <https://doi.org/10.1111/geb.12991>
- 723 Zurell, D., Franklin, J., König, C., Bouchet, P. J., Dormann, C. F., Elith, J., Fandos, G., Feng, X., Guillera-
724 Arroita, G., Guisan, A., Lahoz-Monfort, J. J., Leitão, P. J., Park, D. S., Peterson, A. T., Rapacciuolo,

725 G., Schmatz, D. R., Schröder, B., Serra-Diaz, J. M., Thuiller, W., ... Merow, C. (2020). A standard
726 protocol for reporting species distribution models. *Ecography*, 43(9), 1261–1277.
727 <https://doi.org/10.1111/ecog.04960>

728 Zurell, D., Thuiller, W., Pagel, J., Cabral, J. S., Münkemüller, T., Gravel, D., Dullinger, S., Normand, S.,
729 Schiffers, K. H., Moore, K. A., & Zimmermann, N. E. (2016). Benchmarking novel approaches for
730 modelling species range dynamics. *Global Change Biology*, 22(8), 2651–2664.
731 <https://doi.org/10.1111/gcb.13251>

732